ISSN 0027-1349, Moscow University Physics Bulletin, 2014, Vol. 69, No. 5, pp. 363–373. © Allerton Press, Inc., 2014.
Original Russian Text © S.S. Belyshev, L.Z. Dzhilavyan, B.S. Ishkhanov, I.M. Kapitonov, A.A. Kuznetsov, A.S. Kurilik, V.V. Khankin, 2014, published in Vestnik Moskovskogo Universiteta. Fizika, 2014, No. 5, pp. 3–12.

PHYSICS OF NUCLEI AND ELEMENTARY PARTICLES

Photonuclear Reactions on Titanium Isotopes $^{46-50}$Ti

S. S. Belyshev[a], L. Z. Dzhilavyan[b], B. S. Ishkhanov[a, c], I. M. Kapitonov[a], A. A. Kuznetsov[c], A. S. Kurilik[a], and V. V. Khankin[c]

[a] *Department of Physics, Moscow State University, Moscow, 119991 Russia*
[b] *Institute for Nuclear Research, Russian Academy of Sciences, Moscow, 117312 Russia*
[c] *Skobel'tsyn Institute of Nuclear Physics, Moscow State University, 119991 Russia*
e-mail: kuznets@depni.sinp.msu.ru

Received June 5, 2014; in final form, June 21, 2014

Abstract—Yields of photonuclear reactions on the natural mixture of titanium isotopes were measured under exposure to a beam of bremsstrahlung γ-quanta with the end-point energy of 55 MeV. The results are compared with computations based on the TALYS model. It is shown that description of cross sections of photonuclear reactions on Ti isotopes requires the proper account for isospin and configuration splitting of the giant dipole resonance.

Keywords: photonuclear reactions, radioisotopes, activation analysis, gamma-ray spectroscopy.

DOI: 10.3103/S0027134914050026

INTRODUCTION

The information on cross sections of photonuclear reactions on titanium isotopes is incomplete and has a low accuracy. This work presents the results of measuring the yields of radioisotopes that form in a titanium target of the natural isotopic composition under exposure to bremsstrahlung photons with the end-point energy $E_{\gamma\max} = 55$ MeV. The yields of several photonuclear reactions on the natural mixture of Ti isotopes were measured at this energy for the first time. Cross sections of the (γ, n) and (γ, p) reactions on the even–even Ti isotopes ($A = 46$, 48, and 50) are given. The results are compared with the results of computation based on the TALYS model [1].

1. THE PECULIARITIES OF CROSS SECTIONS AND YIELDS OF INVESTIGATED REACTIONS ON TI ISOTOPES

At present, 26 isotopes of titanium (Ti, atomic number $Z = 22$) are known with mass numbers A from 38 to 63 [2]. Five stable titanium isotopes have the mass numbers $A = 46–50$. Figure 1 displays a part of the $N–Z$ diagram of atomic nuclei (N is the number of neutrons) in the region of Ti stable isotopes. Table 1 presents the percentage of stable isotopes in natural titanium and the thresholds of the (γ, n), (γ, p), (γ, np), $(\gamma, 2n)$, $(\gamma, 2p)$, and $(\gamma, 3n)$ reactions on these isotopes.

For isovector electric giant-dipole resonance (GDR) on Ti isotopes, which is dominant in nuclear photoabsorption cross sections, a fairly complex structure should be expected. The complexity of this structure is determined by the fact that Ti isotopes relate to medium nuclei for which the GDR gross-structure manifestations are essential, which are caused by:

- Nuclei deformation [3, 4];
- Isospin splitting [5];
- Configuration splitting [6].

Investigations of the structure of experimental cross sections of photonucleon reactions on Ti stable isotopes were performed in [7–14]. The main channels of photodisintegration reactions of medium nuclei are (γ, n) and (γ, p). A peculiarity of photonuclear reactions on Ti stable isotopes is that the (γ, n) reactions on all isotopes except for ^{46}Ti do not lead to the formation of radioactive Ti isotopes. As a result, in measurements that use the method of induced activity of targets made of the natural mixture of titanium isotopes [7, 11], the products of photonuclear reactions that form during the emission of protons (above all, of (γ, p) reactions) are mainly recorded. In [7, 11], the induced activity method was used for recording the products of the ^{46}Ti(γ, n) reaction, while in [8–10, 12–14], methods for direct recording of formed photonucleons were applied.

The ^{45}Ti radioisotope can form as a result of ^{A}Ti(γ, xn) reactions on the stable titanium isotopes with the escape of one to five neutrons. When an increase in the mass number, A, of the nucleus-target occurs, two opposite effects are observed. The thresholds of photoneutron reactions are reduced but the photoneutron reaction cross sections also decrease with an increase in the multiplicity of the number of escaping neutrons.

During operation with bremsstrahlung photons, the number of photonuclear reaction acts depends on its yield $Y(E_e)$: convolution of the photonuclear reac-

Table 1. The Ti stable isotopes, the isotope percentage η in the natural mixture, and the thresholds of the indicated reactions on the isotopes $E_{\gamma\,\mathrm{thr}}$ in MeV

Isotope; content in the natural mixture of isotopes η, %	Thresholds of reactions $E_{\gamma\,\mathrm{thr}}$, MeV					
	(γ, *n*)	(γ, *p*)	(γ, *np*)	(γ, 2*n*)	(γ, 2*p*)	(γ, 3*n*)
^{46}Ti; 8.0	13.2	10.3	21.7	22.7	17.2	39.0
^{47}Ti; 7.3	8.9	10.5	19.2	22.1	20.8	31.6
^{48}Ti; 73.8	11.6	11.4	22.1	20.5	19.9	33.7
^{49}Ti; 5.5	8.2	11.4	19.6	19.8	22.8	28.7
^{50}Ti; 5.4	10.9	12.2	22.3	19.1	21.8	30.7

tion cross section $\sigma(E_\gamma)$ with the bremsstrahlung photon spectrum $\phi(E_\gamma, E_e)$:

$$Y(E_e) = \int_{E_{\mathrm{thr}}}^{E_e} \phi(E_\gamma, E_e)\sigma(E_\gamma)dE_\gamma, \qquad (1)$$

where E_e is the kinetic energy of electrons that are incident on the radiator, E_γ is the energy of bremsstrahlung γ-quanta emitted from the radiator, $\phi(E_\gamma, E_e)$ is the spectrum of bremsstrahlung photons that is created in bremsstrahlung of electrons with the kinetic energy E_e in the radiator, and E_{thr} is the threshold of the photonuclear reaction under study.

Computer codes, in particular GEANT4 [15], have been developed that allow the computation of bremsstrahlung photon spectra at high accuracy for different conditions of an experiment.

The yields of photonuclear reactions on bremsstrahlung photon beams $Y(E_e)$ have a number of common features depending on the energy E_e of the electrons that are incident on the radiator:

• $Y(E_e) = 0$ until the threshold of the photonuclear reaction under study is reached, $E_e = E_{\mathrm{thr}}$;

• With the increase $E_e > E_{\mathrm{thr}}$, the yield $Y(E_e)$ grows monotonously;

• After the initial part with the comparatively sharp growth, the yield $Y(E_e)$ transfers to the saturation domain, for which $Y(E_e) \approx \mathrm{const} = Y_{\mathrm{satur}}$.

Measuring the photonuclear reaction yields makes it possible to obtain data on integral cross sections of different-channel reactions of GDR decay in the energy range from 10 to 30 MeV.

2. THE TECHNIQUE AND RESULTS OF MEASUREMENTS

The technique that we use for performing gamma-activation measurements has been described in detail previously [16–18]. This work was carried out at a pulse split microtron [19] on an extracted electron beam with the energy $E_e = 55$ MeV. The electron beam bombarded a tungsten radiator that was 2.1 mm thick [20]. The bremsstrahlung γ-quanta that formed in the radiator irradiated a metallic target-foil 0.06 mm thick made of titanium with the natural isotopic composition. The target was located on the beam axis right against the radiator and almost completely overlapped the bremsstrahlung photon beam. The average electron-beam current during the irradiation process was $I \cong 45.4$ nA. The time of titanium-target irradiation τ was 1 h. After irradiation, the target was transferred to the HPGe spectrometer of γ-quanta. The distance between the irradiated target and the entrance "window" of the HPGe spectrometer was $l \cong 5$ cm. The

Ti43 509 ms β^+	Ti44 63 yr EC	Ti45 184.8 min β^+	Ti46 8.0%	Ti47 7.3%	Ti48 73.8%	Ti49 5.5%	Ti50 5.4%	Ti51 5.76 min β^-
Sc42 0.68 s, 61 s β^+	Sc43 3.891 h β^+	Sc44 3.9 h, 59 h β^+	Sc45 100%	Sc46 83.8 day, 19 s β^+, IT	Sc47 3.3492 day β^-	Sc48 43.67 h β^-	Sc49 57.2 min β^-	Sc50 102.5 s β^-

Fig. 1. The part of the *N*–*Z* diagram of atomic nuclei near stable Ti isotopes. The stable isotopes are marked in black. The value of η, percentage of isotopes in the natural mixture, is indicated for the stable isotopes. The neutron-deficient and neutron-rich radioisotopes are marked in grey and white, respectively. For the radioisotopes (including their isomers), half-life periods and decay modes are indicated.

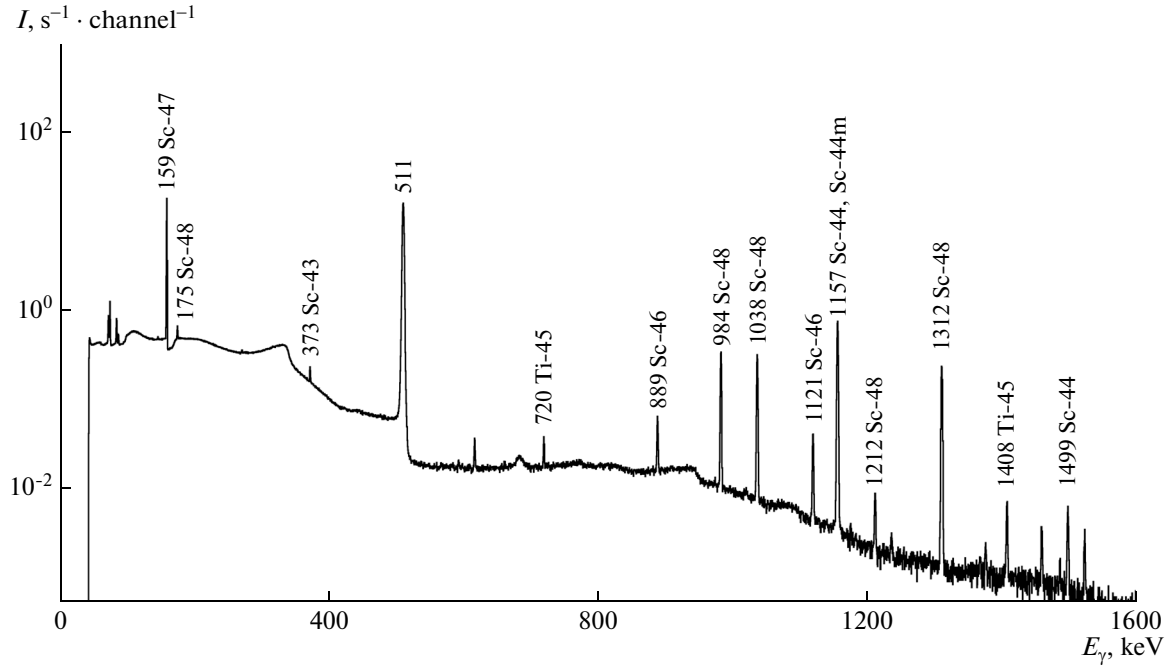

Fig. 2. The γ-quanta spectrum $I(E_\gamma)$ measured from the irradiated Ti sample using the HPGe spectrometer. The inscriptions above the peaks present the energies of the γ-lines (in keV) and the titanium and scandium radioisotopes that correspond to them.

recording of residual activity of the irradiated target began 19 min after the irradiation completion and continued for 9 h.

The activities of different radioisotopes (which were created in the titanium target as a result of irradiation and reduced to the irradiation completion time) were calculated on the basis of analysis of the spectra that were measured by means of the HPGe spectrometer using the γ lines that are characteristic of each radioisotope while taking the quantum-yield values η of these lines into account. The recording efficiency of the HPGe spectrometer for γ-quanta of different energies E_γ was calibrated on the basis of measuring the activity of calibration standard radio sources, as well as performing the simulation with the use of the GEANT4 code [15].

As an example, one of the measured γ-quanta spectra of the decay of the radioisotopes that formed in the irradiated Ti target is shown in Fig. 2.

The observed spectrum peaks from the radionuclides that formed in photonuclear reactions with emission of radionuclide neutrons and protons were identified and compared with the known γ-lines of the appropriate nuclei. Table 2 presents the most intensive γ-lines of the radioisotopes ^{45}Ti, ^{46}Sc, ^{47}Sc, and ^{48}Sc (which formed in the titanium target and was used in processing of the results) and the basic photonuclear reactions leading to formation of these radioisotopes. The large yield of the ^{47}Sc isotope in comparison to other isotopes is caused by the high content of ^{48}Ti in the natural mixture of Ti isotopes.

3. DISCUSSION OF RESULTS

Figure 3 displays the cross sections of photoproton reactions on even–even titanium isotopes: ^{46}Ti(γ, *p*) [7], ^{48}Ti(γ, *p*) [10, 13, 14], and ^{50}Ti(γ, *p*) [9, 12]. The cross sections are obtained in the range of E_γ energies from 10 to 27 MeV. The values of the cross-section maxima are reduced from 37 to 17 mb as the mass number *A* increases from 46 to 50. The values of the integral cross sections

$$\sigma = \int_{10\ \mathrm{MeV}}^{27\ \mathrm{MeV}} \gamma(E_\gamma) dE_\gamma \qquad (2)$$

decrease in this case from 330 [9] to 100 MeV mb [12].

Figure 4 presents the photoneutron-reaction cross sections $\sigma(\gamma, sn) + \sigma(\gamma, 2n) + \sigma(\gamma, pn) + \ldots$ on the isotopes ^{45}Ti [11], ^{48}Ti [13], and ^{50}Ti [12] that were measured within the same energy range. Unlike the photoproton cross sections, the photoneutron cross sections grow as the mass number *A* increases. For the ^{46}Ti isotope, the cross section at the maximum is ≈20 mb; for the ^{48}Ti isotope, it amounts to ≈40 mb and increases to ≈70 mb for the ^{50}Ti isotope. The integral photoneutron reaction cross sections $\sigma(\gamma, sn)$ also grow with an increase in the mass number *A*.

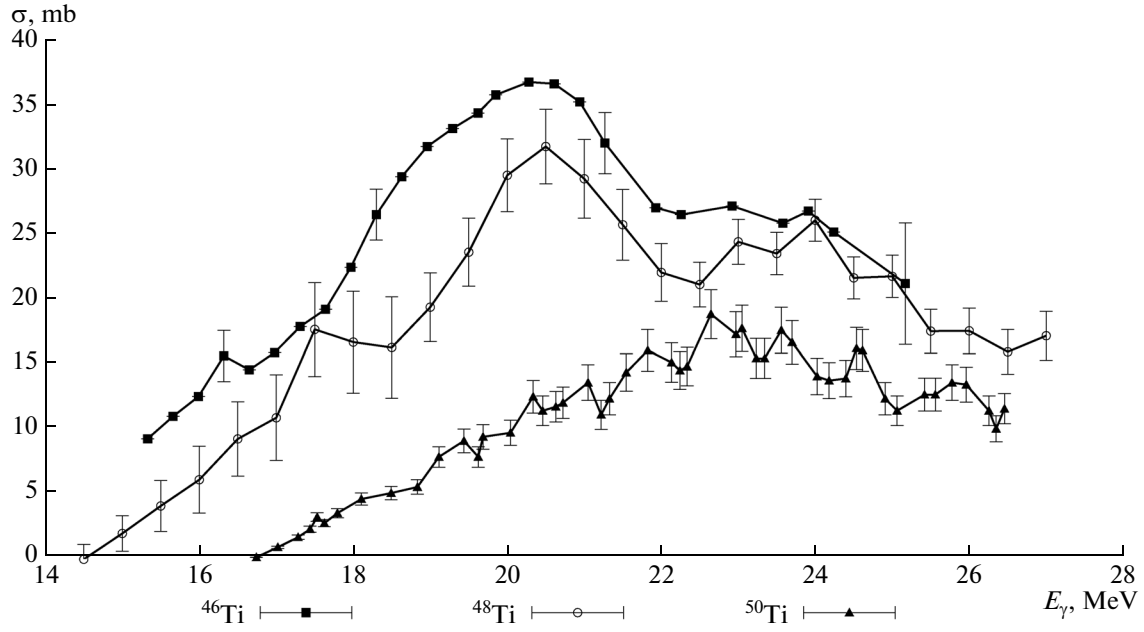

Fig. 3. Experimental cross sections of (γ, *p*) reactions on ^{46}Ti [8], ^{48}Ti [10, 13, 14], and ^{50}Ti [9, 12].

Figure 5 shows the sums σ(γ, *sn*) + σ(γ, *p*) of the experimental cross sections of reactions on the isotopes ^{46}Ti [14], ^{48}Ti [14], and ^{50}Ti [9, 12]. Despite the fact that for individual titanium isotopes the values of the cross sections σ(γ, *sn*) and σ(γ, *p*) differ, the values of the sums of the reaction cross sections σ(γ, *sn*) + σ(γ, *p*) almost coincide for all three isotopes.

Table 3, which is composed on the basis of [7–14] and the photonuclear data atlas [21], contains the information on photonucleon reactions on titanium isotopes obtained using bremsstrahlung photons [7, 11–14] and in reactions of the inelastic decay of electrons [8–10, 14]. While composing Table 5, the following designations for reactions were used:

- σ(γ, *sn*) = σ(γ, *n*) + σ(γ, 2*n*) + σ(γ, *pn*) + ...;
- $E_{\gamma max}$ are the energies corresponding to the maxima of reaction cross sections σ(E_γ);
- σ is the value of the reaction cross section σ(E_γ) at a maximum;

Table 2. The formation of radioisotopes in photonuclear reactions on natural Ti ($T_{1/2}$ is the radioisotope half life, E_γ is the energy of γ-quanta by which the radioisotope identification was performed, η_γ is the quantum yield of the line in the spectrum, Y_{rel} is the radioisotope yield relative to the ^{45}Ti yield)

Radioisotope	Dominating reactions	$T_{1/2}$	E_γ, keV	η_γ	Y_{rel}
^{45}Ti	^{46}Ti(γ, *n*)^{45}Ti	184.8 min	720 1409	0.00154 0.00085	1.0 ± 0.1
^{46}Sc	^{47}Ti(γ, *p*)^{46}Sc+ ^{48}Ti(γ, *pn*)^{46}Sc	83.79 day	889.3 1200.5	0.99984 0.99987	0.95 ± 0.10
^{47}Sc	^{48}Ti(γ, *p*)^{47}Sc	3.3492 day	159	0.683	3.14 ± 0.31
^{48}Sc	^{49}Ti(γ, *p*)^{48}Sc	43.76 h	175 984 1037 1212 1310	0.0748 1.001 0.976 0.0238 1.001	0.18 ± 0.02
^{49}Sc	^{50}Ti(γ, *p*)^{49}Sc	57.2 min	1622.6 1761.97	0.0001 0.0005	0.12 ± 0.03

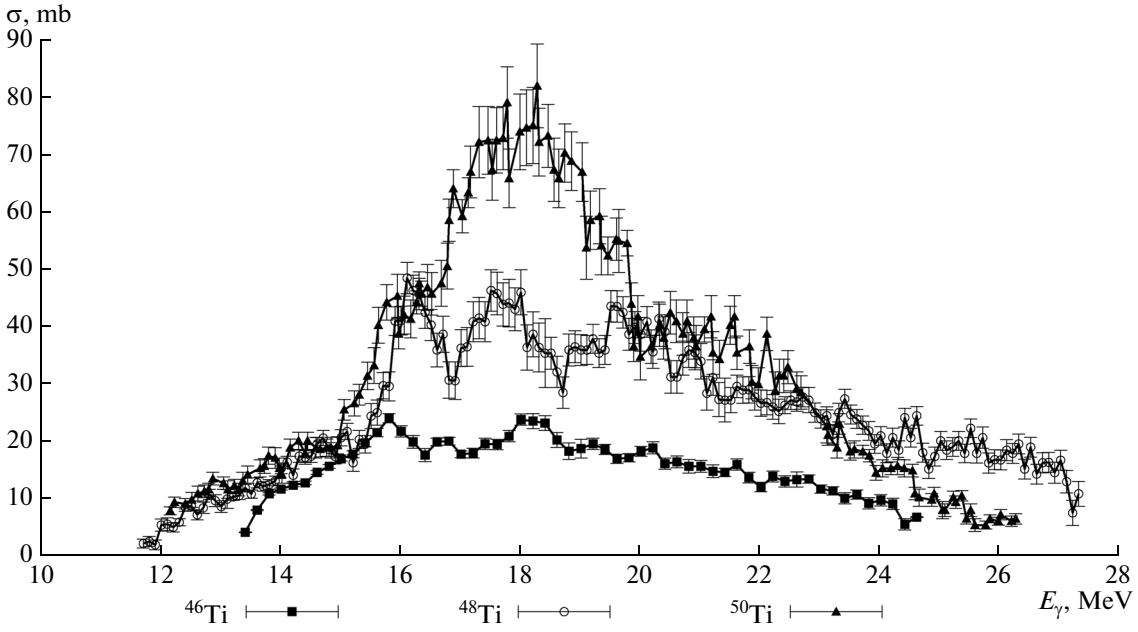

Fig. 4. The experimental cross sections of (γ, *sn*) reactions on ^{46}Ti [11], ^{48}Ti [13], and ^{50}Ti [12].

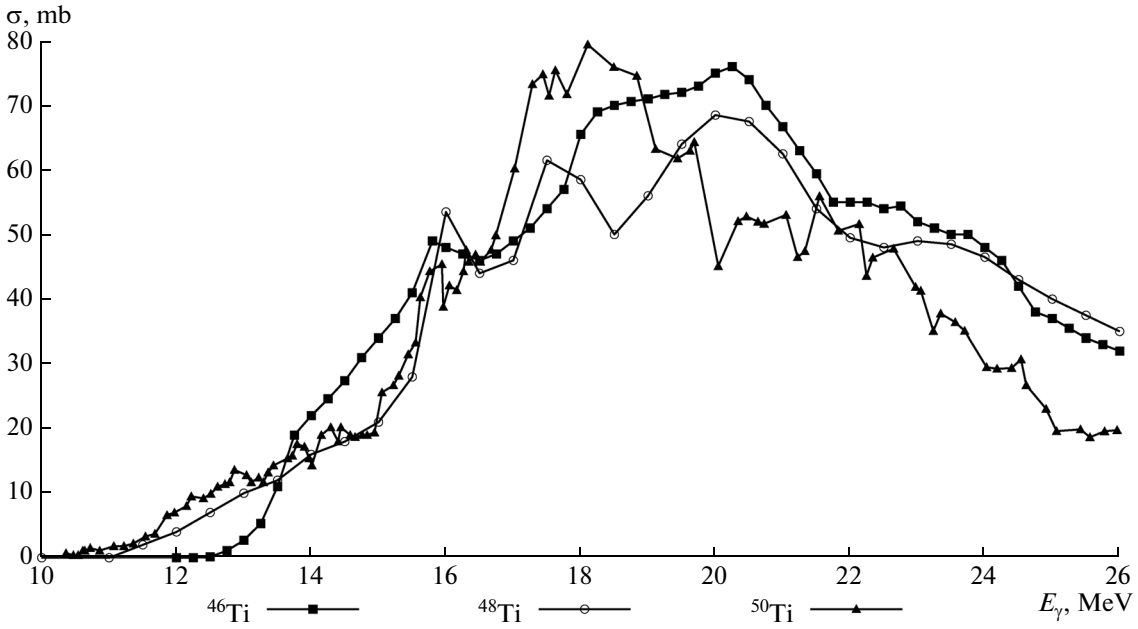

Fig. 5. The sums σ(γ, *sn*) + σ(γ, *p*) of experimental cross sections on ^{46}Ti [14], ^{48}Ti [14], and ^{50}Ti [12].

• FWHM (Full Width at Half Maximum) is the full width at half of the height of the reaction cross section $\sigma(E_\gamma)$;

• E_{int} is the upper limit of integration of the reaction cross section $\sigma(E_\gamma)$ with respect to E_γ;

• σ_{int} is the value of the reaction's integral cross section $\sigma(E_\gamma)$.

As a whole, the shape of the experimental cross sections in Figs. 3–5 is confirmation of the expected complex structure of the GDR of Ti isotopes. The

Table 3. The parameters of the cross sections of photonucleon reactions on Ti isotopes (see designations in the text)

Nucleus–target	Reaction	$E_{\gamma\,max}$, MeV	σ, mb	FWHM, MeV	E_{int}, MeV	σ_{int}, MeV mb	Reference
^{46}Ti	(γ, *n*)	15.8 18	24.13 23.87	8.5	25.0	194	[11]
^{46}Ti	(γ, *sn*)	20.5	31	8.5	31.0	269	[11]
^{46}Ti	(γ, *p*)	20.2	37	9	25.5	333	[8]
^{48}Ti	(γ, *sn*)	16.1 17.5 19.5	48.55 46.36 43.64	7.5	27.0	398	[13]
^{48}Ti	(γ, *p*)	21 24	30 25	11.5	29.0	345	[10, 13, 14]
^{50}Ti	(γ, *sn*)	18.27 21.56	75 40	7	26.3	473	[12]
^{50}Ti	(γ, *sn*)	23	16	6	26.3	96	[9, 12]

Table 4. The integral cross sections $\sigma_{int}(\gamma, sn)$ and $\sigma_{int}(\gamma, p)$ of the reactions on the stable even–even titanium isotopes ^{46,48,50}Ti that were obtained from experiments and computations using the TALYS code. The percentage indicates the exhaustion of the dipole rule of sums

Isotope of titanium ($Z = 22$)	Experiment			Computation using the TALYS code		
	$\sigma_{int}(\gamma, sn)$, MeV mb	$\sigma_{int}(\gamma, p)$, MeV mb	$\sigma_{int}(\gamma, sn) + \sigma_{int}(\gamma, p)$, MeV mb	$\sigma_{int}(\gamma, sn)$, MeV mb	$\sigma_{int}(\gamma, p)$, MeV mb	$\sigma_{int}(\gamma, sn) + \sigma_{int}(\gamma, p)$, MeV mb
^{46}Ti	269 [11]	333 [8]	602 (87%)	275	270	545 (78%)
^{48}Ti	398 [13]	345 [10]	743 (104%)	554	104	658 (92%)
^{50}Ti	473 [12]	96 [9]	569 (77%)	709	9	718 (98%)

comparison of the reaction cross sections σ(γ, *n*), σ(γ, *p*), and σ(γ, *n*) + σ(γ, *p*) on ^{46}Ti, ^{48}Yi, and ^{50}Ti isotopes with the cross sections on the double magic nucleus ^{40}Ca [21] shows a substantial role of isospin splitting and the configuration splitting of GDR on Ti isotopes. In particular, this follows from the comparison of GDR widths for the ^{40}Ca isotope and $^{46, 48, 50}$Ti isotopes. The cross sections of reactions on ^{40}Ca have characteristic values of full width at a half height (FWHM) of ≈5 MeV, whereas the FWHM values on $^{46, 48, 50}$Ti isotopes increase by approximately twofold. However the reliable discrimination of the isotopic and configuration splitting of GDR in Ti isotopes is difficult due to the mutual superposition of these effects.

Table 5. The isospin splitting of GDR in the ^{46,48,50}Ti isotopes

Isotope	Δ*E*, MeV	$s(T_>)/s(T_<)$
^{46}Ti	2.6	0.79
^{48}Ti	3.7	0.35
^{50}Ti	4.8	0.20

For analysis of obtained results for photonuclear reaction cross sections, the cross sections of reactions on titanium isotopes were computed using the TALYS1.6 code [1].

Figure 6 displays the computed reaction cross sections σ(γ, *n*), σ(γ, 2*n*), σ(γ, *p*), σ(γ, 2*p*), and the total cross section σ(γ, abs) = σ(γ, *n*) + σ(γ, 2*n*) + σ(γ, *p*) + σ(γ, 2*p*) for the $^{46–50}$Ti isotopes. A peak at $E_\gamma \approx$ 12.5 MeV in the ^{46}Ti(γ, *p*) reaction cross section is connected with the threshold effect: competition between the channel of GDR decay with proton emission and the opening channel of GDR decay with neutron emission.

Table 4 presents the integral cross sections $\sigma_{int}(\gamma, sn)$, $\sigma_{int}(\gamma, p)$, and $\sigma_{int}(\gamma, n) + \sigma_{int}(\gamma, p)$ on the stable even–even Ti isotopes that were computed using the TALYS code. The analysis of model computations shows the following regularities in the reaction cross sections:

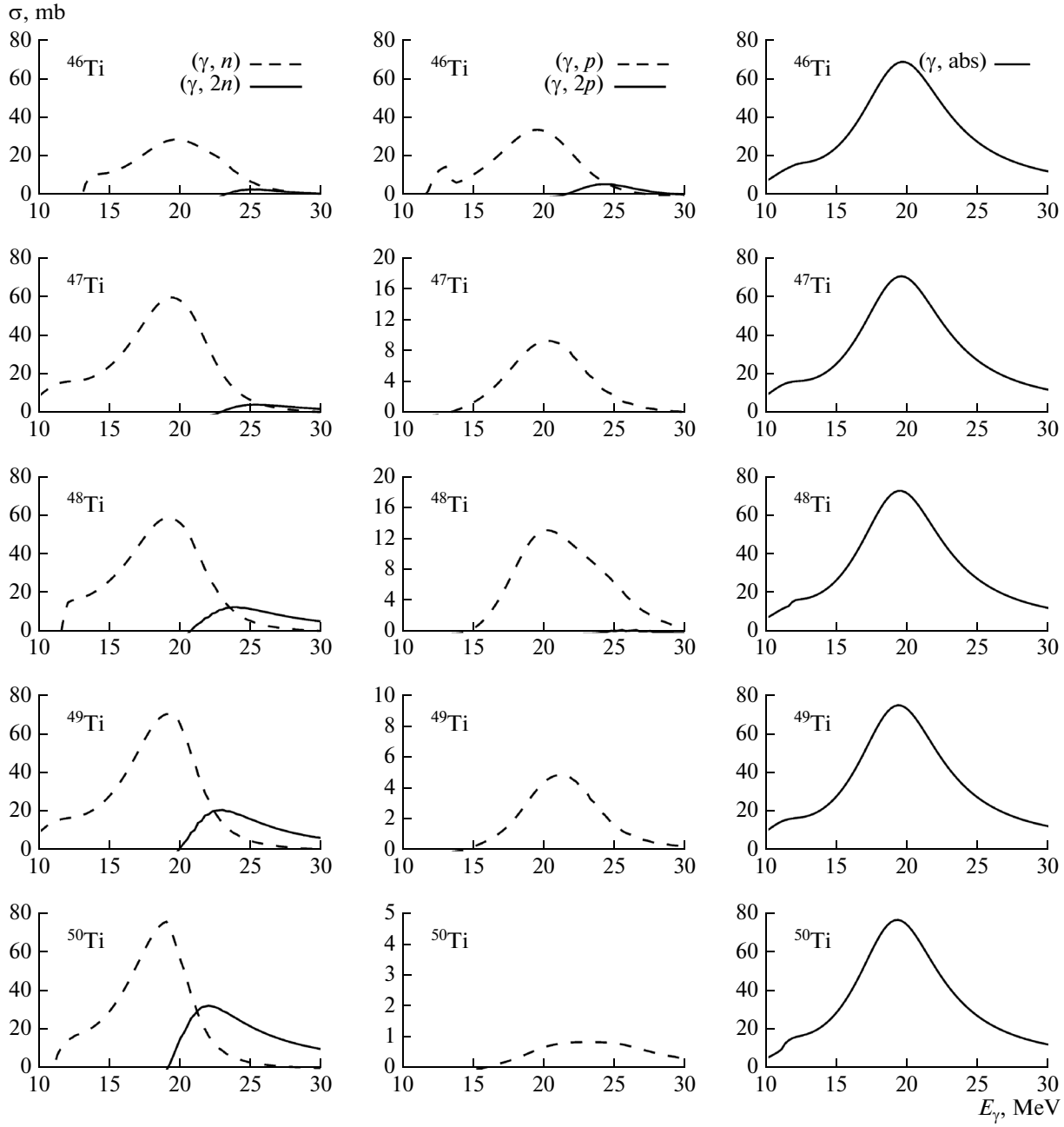

Fig. 6. The cross sections of photonuclear reactions on the titanium isotopes $^{46-50}$Ti computed on the basis of the TALYS code [1]. The first column of plots shows the photoneutron reaction cross sections $\sigma(\gamma, n)$ (dashed lines) and $\sigma(\gamma, 2n)$ (solid lines). In the second column of plots, the photoproton reaction cross sections $\sigma(\gamma, p)$ (dashed lines) and $\sigma(\gamma, 2p)$ (solid lines) are presented. The third column of plots displays the total photoabsorption cross sections $\sigma(\gamma, \text{abs}) = \sigma(\gamma, n) + \sigma(\gamma, 2n) + \sigma(\gamma, p) + \sigma(\gamma, 2p)$ on the isotopes $^{46-50}$Ti.

• The integral reaction cross sections $\sigma_{\text{int}}(\gamma, sn)$ grow with an increase in the mass number A;

• The integral reaction cross sections $\sigma_{\text{int}}(\gamma, p)$ decrease with an increase in the mass number A;

• The sum of integral cross sections $\sigma_{\text{int}}(\gamma, n) + \sigma_{\text{int}}(\gamma, p)$ also increases as the mass number A grows. This increase in the integral cross section occurs due to the growth in the cross section $\sigma_{\text{int}}(\gamma, sn)$.

The results of computations using the TALYS code are juxtaposed in Table 4 with experimental data. Their comparison indicates a strong discrepancy between them and the experimental data. First, this is revealed in the description of photoproton cross sec-

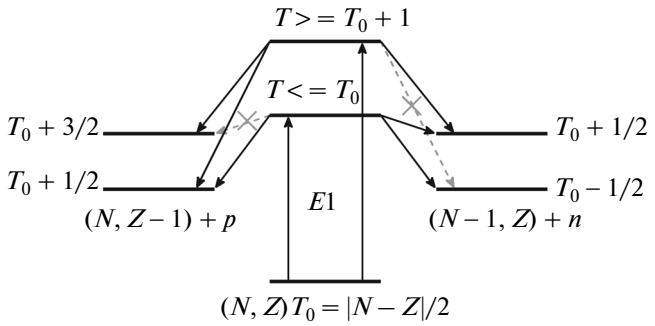

Fig. 7. The excitation and decay of the $T_> = T_0 + 1$ and $T = T_0$ states in nuclei with $N \neq Z$ with absorption of $E1$ γ quantum.

tions. If in the case of the ^{46}Ti isotope, the model computations agree with experimental data at an accuracy of 10%, then with an increase in the mass number A, the difference between the experiment and the model description of cross sections grows. In the case of the ^{48}Ti isotope, the integral cross section $\sigma_{int}(\gamma, p)$ is three times smaller than the experimentally measured one. In the ^{50}Ti case, the distinction in integral cross sections is increased tenfold. The experimentally measured cross section amounts to 96 MeV mb, whereas the theoretically computed cross section is only 9 MeV mb.

The cause of this difference in the description of experimental data is that the isospin splitting of GDR is not taken into account in the TALYS code. The effect of the GDR isospin splitting consists in the fact that in the nuclei with $N \neq Z$ when dipole electric γ-quanta are absorbed, two GDR branches are excited: with an isospin of $T_< = T_0$ and $T_> = T_0 + 1$, where $T_0 = (N - Z)/2$. The value of GDR isospin splitting and the ratio of channels of GDR decay (with emitting protons and neutrons) depend on the T_0 isospin value of the initial nucleus in the ground state (Fig. 7).

The value of GDR isospin splitting ΔE in nuclei with $N \neq Z$ [5] is described by the relationship

$$\Delta E = \frac{60}{A}(T_0 + 1)\ \text{MeV}. \qquad (3)$$

In $^{46, 48, 50}$Ti isotopes, the T_0 isospin value grows from 1 to 3, which leads to an increase in the value of GDR isospin splitting on the $^{46, 48, 50}$Ti isotopes from 2.6 to 4.8 MeV as the mass number A increases.

The probability of the excitation of the $s(T_>)$ and $s(T_<)$ states [5] is described by the relationship

$$\frac{s(T_>)}{s(T_<)} = \frac{1}{T_0}\frac{1 - 1.5\,T_0 A^{-2/3}}{1 + 1.5A^{-2/3}}. \qquad (4)$$

The ratio $s(T_>)/s(T_<)$ for $^{46, 48, 50}$Ti isotopes reduces from 0.79 to 0.20 as the mass number A increases. Thus, in the even–even $^{46, 48, 50}$Ti isotopes, GDR isotopic splitting occurs with an increase in the mass number, A; however, the relative role of the $s(T_>)$ excitation channel decreases in this case.

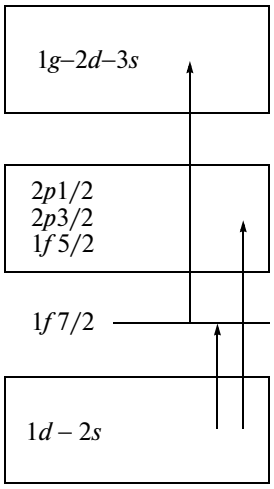

Fig. 8. The configuration splitting of the GDR of Ti isotopes.

The neutron-channel decay of the $T_>$ state to states of the nucleus $(N-1, Z)$ is forbidden by the isospin selection rule, which increases the probability of the $T_>$ state decay by proton channel and thus extends the (γ, p) reaction cross section. The neglect of the specificity of the state proton-channel decay in the TALYS code results in the incorrect ratio between the (γ, sn) and (γ, p) reactions cross sections: a reduction in the (γ, p) reaction cross section leads to growth in the (γ, sn) reaction cross section. The characteristics of isospin splitting of Ti isotopes are given in Table 5. The isospin splitting of GDR on Ti isotopes is clearly revealed in the (γ, p) reaction cross sections that are

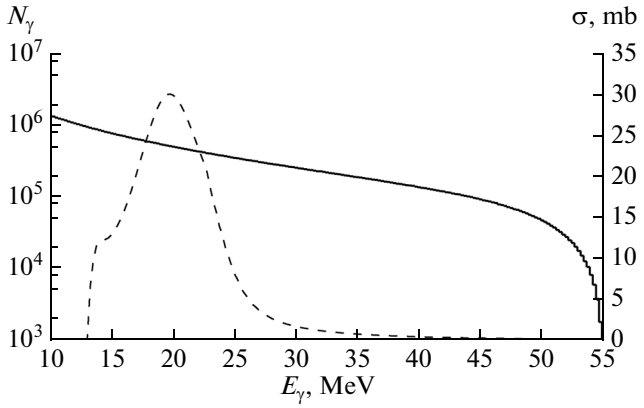

Fig. 9. The spectrum of bremsstrahlung photons from a tungsten radiator 2.1 mm thick at $E_e = 55$ MeV (solid line), which was computed using the GEANT4 code [15], and the ^{46}Ti$(\gamma, n)^{45}$ cross section (dashed line), as computed on the TALYS code basis [1].

Table 6. Comparison of the relative yields Y_{rel} of photonuclear reactions on the natural mixture of titanium isotopes that were obtained in this work with computations using the TALYS code. The photonuclear reaction yields are normalized to the ^{45}Ti yield. The integral cross sections σ_{int} of photonuclear reactions on stable titanium isotopes that were computed using the TALYS code in the energy range up to 55 MeV. The relative cross sections $\sigma_{int\ rel}$ are normalized to the ^{45}Ti cross section and the percentage of appropriate isotopes in the natural mixture of Ti isotopes

Isotope	Reaction	This work	TALYS		
		Y_{rel}	Y_{rel}	$\sigma_{int\ rel}$	σ_{int}, MeV mb
^{45}Ti	^{46}Ti(γ, n) + ^{47}Ti($\gamma, 2n$)	1.06 ± 0.1	1.0	1.0	265.8 + 62.9
^{45}Sc	^{46}Ti(γ, p) + ^{47}Ti(γ, pn) + ^{48}Ti($\gamma, p2n$)		1.39	2.21	277.3 + 139.3 + 33.4
^{46}Sc	^{47}Ti(γ, p) + ^{48}Ti(γ, pn)	0.95 ± 0.10	0.84	1.74	74.6 + 53.7
^{47}Sc	^{48}Ti(γ, p)	3.14 ± 0.30	2.97	3.12	109.2
^{48}Sc	^{49}Ti(γ, p) + ^{50}Ti(γ, pn)	0.18 ± 0.02	0.085	0.12	37.7 + 19.1
^{49}Sc	^{50}Ti(γ, pn)	0.12 ± 0.03	0.019	0.027	12.7

given in Fig. 3. The maximum of the cross section of the (γ, p) reaction on ^{50}Ti isotope is shifted with respect to the maximum of the cross section of the (γ, p) reaction on ^{46}Ti isotope by approximately 2 MeV towards the higher energies in accordance with Eq. (3).

In $^{46-50}$Ti isotopes, filling the $1f_{7/2}$ subshell with neutrons occurs as the mass number A increases, which leads to GDR configuration splitting (Fig. 8). The filling of the neutron $1f_{7/2}$ subshell reduces the probability of the $(1d, 2s) \longrightarrow 1f_{7/2}$ transitions and increases the probability of the $1f_{7/2} \longrightarrow (1g, 2d, 3s)$ transitions. Another factor that influences the ratio of GDR decays with emission of protons and neutrons is the increase in the (γ, p) reaction threshold and decrease in the (γ, n) reaction threshold with the A mass number growth in Ti isotopes (see Table 1).

The experimental and computed values of the total reaction cross sections $\sigma_{int}(\gamma, sn)$ and $\sigma_{int}(\gamma, p)$ for even–even $^{46, 48, 50}$Ti isotopes in Table 4 are compared with the prediction of the dipole sum rule [22]

$$\sigma_{int} = 60\frac{NZ}{A}, \quad (5)$$

which yields the values 690, 715, and 740 Mev mb, respectively, for these isotopes.

From the analysis of data given in Table 4, it follows that the accuracy of the measured photoproton and photoneutron reaction cross sections does not exceed 20% and the data need refinement.

The sum of the values of the integral reaction cross sections $\sigma_{int}(\gamma, n)$ and $\sigma_{int}(\gamma, p)$ that are given in Table 4 is ≈85% of the dipole sum rule, which is evidence of the dominating role of these channels of GDR decay for the atomic nuclei domain under study.

The maxima of the cross sections of photonuclear reactions on Ti isotopes are located in the vicinity of the energy ≈20 MeV. However, the reaction cross sections continue to the range of higher energies. The values of the integral photonuclear reaction cross sections that were computed using the TALYS code within the energy range of 25–55 MeV amount to ≈15% of the total cross section of γ-quanta absorption. In this energy range, the quasi-deuteron mechanism of γ-quanta absorption plays a definite role, together with GDR.

In this experiment, the yields of several photonuclear reactions on Ti isotopes within the energy range to 55 MeV were obtained using the γ-activation technique. The results are given in Tables 2 and 6. An advantage of the gamma-activation experiment is that yields of photonuclear reactions on different isotopes are measured in a single experiment, which reduces relative errors in comparing the yields of different reactions. Figure 9 shows the bremsstrahlung γ-quanta spectrum (computed using GEANT4 [15]), with which the irradiations were conducted in this experiment. The shape of the bremsstrahlung γ-quanta spectrum with the end-point energy $E_e = 55$ MeV changes weakly (≈20%) in the vicinity of the maxima of cross sections of photonucleon reactions on Ti isotopes. Therefore, the ratio of the reaction yields can be juxtaposed with values of the integral reaction cross sections at an accuracy of 20%:

$$\frac{Y_1(E_e)}{Y_2(E_e)} = \frac{\int_{E_{thr}}^{E_e} \Phi(E_\gamma, E_e)\sigma_1(E_\gamma)dE_\gamma}{\int_{E_{thr}}^{E_e} \Phi(E_\gamma, E_e)\sigma_2(E_\gamma)dE_\gamma} \approx \frac{\int_{E_{thr}}^{E_e} \sigma_1(E_\gamma)dE_\gamma}{\int_{E_{thr}}^{E_e} \sigma_2(E_\gamma)dE_\gamma} \approx \frac{\sigma_{1int}}{\sigma_{2int}}. \quad (6)$$

In Table 6, the data we obtained on photonuclear-reaction yields are compared to theoretical computations with the use of the TALYS code. The first column of Table 6 presents the isotopes that formed as a result of irradiating the target of the natural mixture of Ti isotopes. Basic reactions that make a contribution to the formation of a given isotope are included in the second column of Table 6. The third column of Table 6 contains the yields of the isotopes that we measured (normalized to the ^{45}Ti isotope yield). The sixth column presents integral cross sections of appropriate reactions in the range of energies up to 55 MeV. The experiment results are compared to computations based on the TALYS code. The fifth column of Table 6 includes the integral cross sections that were computed using the TALYS code that are normalized to the integral cross section of reactions that lead to formation of ^{45}Ti. The third and fourth columns present the relative yields of isotopes (created as a consequence of irradiation of the target made of the natural mixture of Ti isotopes) that were obtained experimentally and as a result of computation using the TALYS code. All yields are normalized to the ^{45}Ti yield.

The comparison of our experimental data with computations using the TALYS code shows that the basic experimental regularities are conveyed correctly as a whole. The photoproton reaction yields decrease as the mass number A increases. However, unlike the experimental data, the reduction in theoretically computed yields occurs much more sharply. As we already noted above, this is caused by the fact that the GDR isospin splitting is not taken into account in the TALYS code.

The largest difference between the yields and relative integral cross sections computed using the TALYS code is observed for the ^{45}Sc and ^{46}Sc isotopes. The large relative integral cross section of formation of these isotopes is associated with the contribution from the cross section of reactions on the ^{48}Ti isotope, the content of which in the natural mixture is 73.8%.

CONCLUSIONS

For the first time, yields of several photonuclear reactions on the natural mixture of Ti isotopes were measured in the range of γ-quanta energies up to 55 MeV. From comparison of the available experimental data with theoretical computations using the TALYS code, it follows that the main channels of photonuclear reactions on the ^{46}Ti isotope are the channels of reactions with the emission of protons and neutrons. With an increase in the mass number, A, the (γ, p) reaction cross section decreases sharply and amounts to approximately 20% of the total absorption cross section for the ^{48}Ti isotope. For the ^{50}Ti isotope, the photonuclear reaction cross section is ≈1% of the total absorption cross section. The value of the total integral cross section of photonuclear reactions in the energy range up to 30 MeV on Ti isotopes is $\sigma_{int}(30\ \text{MeV}) = 650 \pm 50$ MeV mb, which exhausts ≈85% of the dipole sum rule.

The isospin splitting and configuration splitting of GDR play a substantial role in the description of GDR excitation and decay leading to an increase in the width of giant resonance on Ti isotopes as compared to the neighboring double magic nucleus, ^{40}Ca. The presently obtained experimental data as a whole provide the description of the main features of the GDR excitation and decay on Ti isotopes. However, the diversity of conceptual problems of GDR description requires more accurate experimental data. In particular, it is interesting (i) to study the influence of paired protons at the $1f_{7/2}$ shell on the neutron population of Ti outer shells, (ii) to investigate the impact of the population of $1f_{7/2}$ outer shells on the Fermi-surface blurring, and (iii) to trace the formation of the magic number $N = 28$.

REFERENCES

1. A. J. Konig, S. Hilaire, and M. C. Duijvestijn, *Proc. Int. Conf. on Nuclear Data for Science and Technology, 2007*, Ed. by O. Bersillon, (EDP Sci., Nice, 2008).
2. L. P. Ekstrom and R. B. Firestone, http://ie.lbl.gov/toi/
3. K. Okamoto, Phys. Rev. **110**,143 (1958).
4. M. Danos, Nucl. Phys. A: Nucl. Handron. Phys. **5**, 23 (1958).
5. S. Fallieros and B. Goulard, Nucl. Phys. A: Nucl. Handron. Phys. **147**, 593 (1970).
6. R. A. Eramzhyan, B. S. Ishkhanov, I. M. Kapitonov, and V. G. Neudatchin, Phys. Reports **136**, 229 (1986).
7. T. R. Scherwood and W. E. Turchinetz, Nucl. Phys. A: Nucl. Handron. Phys. **29**, 292 (1962).
8. S. Oikawa and K. Shoda, Nucl. Phys. A: Nucl. Handron. Phys. **277**, 301 (1977).
9. M. N. Thompson, K. Shoda, M. Sugavara, et al., Reserch Report of Laboratory of Nuclear Science, Tohoku University, **10**, 55 (1977).
10. J. Weise, et al., Research Report of Laboratory of Nucl. Sci. Tohoku University, **11**, 43 (1978).
11. R. E. Pywell and M. N. Thompson, Nucl. Phys. A: Nucl. Handron. Phys. **318**, 461 (1979).
12. R. E. Pywell, M. N. Thomspon, and R. A. Hicks, Nucl. Phys. A: Nucl. Handron. Phys. **325**, 116 (1979).
13. R. Sutton, M.N. Thompson, M. Sugawara, K. Shoda, T. Saito, and H. Tsubotaet, Nucl. Phys. A: Nucl. Handron. Phys. **339**, 125 (1980).
14. B. S. Ishkhanov, I. M. Kapitonov, E. I. Lileeva, E. V. Shirokov, V. A. Erokhova, M. A. Elkin, and A. V. Izotova, Cross sections of photon absorption by nuclei with nucleon numbers 12–65, *Preprint Inst. Nucl. Phys. Mos. State Univ.*, Moscow, 2002, no. 2002/711.

15. S. Agostinelli, J. Allison, K. Amako, J. Apostolakis, H. Araujo, P. Arce, M. Asai, D. Axen, S. Banerjee, G. Barrand, F. Behner, L. Bellagamba, J. Boudreau, L. Broglia, A. Brunengo, H. Burkhardt, S. Chauvie, J. Chuma, R. Chytracek, G. Cooperman, and G. Cosmo, Nucl. Instr. Meth. Phys. Res. A: Accel., Spectr., Detect., Assoc. Equip. **506**, 250 (2003).

16. S. S. Belyshev, B. S. Ishkhamov, L. Z. Dzhilavyan, A. N. Ermakov, V. V. Khankin, V. I. Shvedunov, A. I. Kartev, and V. G. Raevsky, Mos. Univ. Phys. Bull. **67** (3), 246 (2012).

17. S. S. Belyshev, L. Z. Dzhilavyan, A. N. Ermakov, V. V. Khankin, A. A. Kuznetsov,V. I. Shvedunov, and K. A. Stopani, Bull. Russ. Acad. Sci.: Phys. **77** (4), 480 (2013).

18. S. S. Belyshev, A. N. Ermakov, B. S. Ishkanov, V. V. Khankin, A. S. Kurilik, A. A. Kuznetsov, V. I. Shvedunov, and K. A. Stopani, Nucl. Instrum. Methods Phys. Res., Sect. A: Accel., Spectr., Detect., Assoc. Equip. **745**, 133 (2014).

19. A. I. Karev, A. N. Lebedev, V. G. Raevsky, et al., *Proc. 22nd Russ. Particle Acceler. Conf. (RuPAC-2010)*, 316 (2010).

20. S. M. Seltzer and M. J. Berger, Nucl. Instr. Meth. Phys. Res. B: Beam Interac. Mater. Atoms **12**, 95 (1985).

21. A. V. Varlamov, V. V. Varlamov, D. S. Rudenko, and M. E. Stepanov, Atlas of Giant Dipole Resonances. Parameters. and Graphs of Photonuclear Reaction Cross Sections. INDC (NDC), Vienna, Vol. 394, (1999).

22. B. S. Ishkhanov and I. M. Kapitonov, *Vzaimodeistvie elektromagnitnogo izlucheniya s atomnymi yadrami* (Interaction of Electromagnetic Radiation with Atomic Nuclei) (Moscow, 1979) [in Russian].

Translated by M. Samokhina